

25th ABCM International Congress of Mechanical Engineering
October 20-25, 2019, Uberlândia, MG, Brazil

VIBRATIONAL ANALYSIS OF POWER TRANSMISSION TOWER BY SPECTRAL ELEMENT METHOD: A NUMERICAL VALIDATION

Yanne Marcela Soares Fernandes

Marcela Rodrigues Machado

University of Brasilia, Brasilia, Brazil.

yannemarcela@hotmail.com

Maciej Dutkiewicz

University of Science and Technology, Bydgoszcz, Poland.

macdut@utp.edu.pl

Edilson Dantas Nóbrega

Federal University of Maranhao, Sao Luiz- MA, Brazil

edilsonnobre@gmail.com

Abstract. *This paper presents a study of power transmission self-supporting tower using the Spectral Element Method (SEM), to facilitate the analysis with a lower discretisation of the elements. The numerical analysis performed through computational implementation investigates the vibrational response of the tower. The results are validated by comparing them with results obtained via the Finite Element Method (FEM). Due to SEM is formulated based on the exact solution method, no need to discretize the continuous elements, which implies in the low computational effort and time-consuming. The vibration response of the tower obtained by SEM and FEM are presented, and the cost involved in both approaches computed.*

Keywords: *Transmission tower, dynamic analysis, spectral element method.*

1. INTRODUCTION

In many countries, as in Brazil, electric energy travels long distances from the generation points to the final consumer, which requires a large demand for energy transmission systems. As the weight and extension of transmission systems increases, the need for safety and reliability of these structures increases (Yasui, Marukawa, Momomura, & Ohkuma, 1999). The towers are responsible for supporting their weight, the cables and its dynamic behaviour, besides other random loads due to rain and wind gusts. Thus, turning the dynamic analysis of the system a complicated process. In the operational situations, the forces of the transmission cables cannot be neglected, it because those structures are subject to accumulated damages, and in general, a cascade effect occurs due to failures of successive towers.

Transmission towers have been studied over decades, Naidu and Krishna (2016) presented a numerical study determined the static response for wind loads in a vertical and transverse position, and a modal and dynamic analysis due to variable wind load over time. Lam and Yin (2011) investigate damage detection methods applied to a laboratory-scale or reduced-scale tower model. Taillon et al. (2012) performed a comparison between experimental and numerical results to evaluate the relationship between rigidity and damping for structures requested in the different solicitation. Prasad Rao et al. (2010) carried out tests on large-scale structures and compared them with a numerical model to predict failure patterns and final load.

The Spectral Element Method (SEM) is a mesh method similar to the FEM, in which the approximate form functions of the element are replaced by functions of the exact dynamic form obtained from the correct solution of differential equations of government. In this way, a single element is sufficient to model any continuous and uniform part of the structure. This feature reduces significantly the number of elements required in the design model and improves the accuracy of the dynamic system solution. The extensive study of the fundamentals and a variety of new applications of SEM, such as composite laminated, periodic truss, smart material was presented in (Doyle, 1997; Lee, 2009). The behaviour of the waves in composites and inhomogeneous media were studied by Gopalakrishnan et al. (2007). Studies related to the detection of structural damage was developed by Palacz et al. (2002), and an extensive approach to elementary and high order rod was carried out in Pereira (2009) and Krawczuk et al. (2006).

The SEM has some disadvantages when compared to FEM as unavailability of exact wave solutions for more complex 2D and 3D structures. In such cases, approximate modelling of different components can be used and can still provide very accurate solutions. However, SEM guarantees an accurate response in the frequency domain. In this paper, a study of power transmission self-supporting tower using the SEM is presented. The main goal is overcoming the numerical analysis to investigate the vibrational response of the tower. The results are validated by comparing with the

result obtained by the FEM. The vibration response of the tower obtained by SEM and FEM are presented, and the computational cost involved in both approaches analysed.

2. SPECTRAL ELEMENT METHOD

2.1 The spectral element of the elementary rod

The elementary rod model, which was used in this work to develop the truss, considers only axial loads and does not consider the Poisson effect, in this way the deformations are only unidimensional. Figure 1 shows the elementary rod element with two nodes having a force and a displacement by the node.



Figure 1.Elementary rod

The equation of motion for an undamped rod is given by,

$$EA_s \left(\frac{\delta^2 u_{x,t}}{\delta x^2} \right) - \rho A_s \left(\frac{\delta^2 u_{x,t}}{\delta t^2} \right) = 0. \quad (1)$$

where the parameter E is the Young's Modulus of the material, A_s is the cross section of the element, ω is the angular frequency, u is the longitudinal displacement, and F is the excitation force. In the spectral form of the movement equation can be described as,

$$\frac{E_c A_s (\delta^2 \hat{u})}{\delta x^2} + \omega^2 \rho A_s \hat{u} = 0, \quad (2)$$

where $\hat{\cdot}$ is the indication of the Fourier transform, $E_c = E(1 + i\eta)$ represents the complex Young's Modulus and structural damping, and η is the loss factor. The homogeneous solution based on the wave propagation is expressed as,

$$\hat{u}_x = A_1 e^{-ikx} + A_2 e^{-it(L-x)}, \quad (3)$$

A_1 and A_2 are constants, L is the rod length, and k is the wavenumber given by,

$$k = \omega \sqrt{\frac{\rho}{E_c}}. \quad (4)$$

The boundary conditions for the displacement are expressed as,

$$\hat{u}_0(x=0) = A_1 + A_2 e^{-ikL} \quad (5)$$

$$\hat{u}_L(x=L) = A_1 e^{-ikL} + A_2$$

and the axial force in the rod is given by,

$$\hat{F}_x = E_c A_s \frac{\delta u}{\delta x} \quad (6)$$

By rewriting the nodal displacements in the matrix form, it was obtained the spectral dynamic stiffness matrix $K(\omega)$ of the elementary rod (Doyle, 1997),

$$K(\omega) = \frac{EA}{L} \frac{ikL}{(1 - e^{-i2kL})} \begin{bmatrix} 1 + e^{-i2kL} & -2e^{-i2kL} \\ -2e^{-i2kL} & 1 + e^{-i2kL} \end{bmatrix}. \quad (7)$$

2.2. The spectral element of the Loverod

The Loveand elementary rod haveonly one degree of freedom and subject only to axial forces, as shown in Fig.1. However, Love's theory takes into account the Poisson effect (ν);it considers that the longitudinal deformation causes a transversal effect, and the equation of motion will be,

$$EA_s \left(\frac{\delta^2 u_{x,t}}{\delta x^2} \right) - \rho A_s \left(\frac{\delta^2 u_{x,t}}{\delta t^2} \right) + \nu^2 \rho J \frac{\delta^2}{\delta x^2} \left(\frac{\delta^2 u_{x,t}}{\delta t^2} \right) = 0 \quad (8)$$

By rewriting in the spectral form,it has,

$$EA_s \left(\frac{\delta^2 \hat{u}}{\delta x^2} \right) + \rho A_s \omega^2 \hat{u} - \nu^2 \omega^2 \rho J \frac{\delta^2 \hat{u}}{\delta x^2} = 0 \quad (9)$$

$$F = (EA_s - \nu^2 \omega^2 \rho J) \frac{d\hat{u}}{dx} \quad (10)$$

where J is the polar moment of inertia of the cross section of the element.It will be also considered structural damping included in the structural parameter Young's modulus.Since k_l is the wave number for the Love rod given by equation.

$$k_{lo} = \pm \omega \sqrt{\frac{\rho A_s}{EA_s - \nu^2 \rho J \omega^2}} \quad (11)$$

The longitudinal displacement obtained through the homogeneous solution is given by

$$\hat{u}_x = A_1 e^{-ik_{lo}x} + A_2 e^{-ik_{lo}(L-x)}, \quad (12)$$

By applying the boundary conditions in the displacement and considering x equal to 0 and L we have,

$$\begin{aligned} \hat{u}_0 &= A_1 + A_2 e^{-ik_{lo}L} \\ \hat{u}_L &= A_1 e^{-ik_{lo}L} + A_2 \end{aligned} \quad (13)$$

which can be represented by the matrix as,

$$\begin{Bmatrix} A_1 \\ A_2 \end{Bmatrix} = \underbrace{\begin{bmatrix} 1 & e^{-ik_{lo}L} \\ e^{-ik_{lo}L} & 1 \end{bmatrix}}_{\Gamma}^{-1} \begin{Bmatrix} \hat{u}_0 \\ \hat{u}_L \end{Bmatrix} \quad (14)$$

With the application of the boundary conditions in the forces and considering that F_1 and F_2 are the forces applied on the nodes at a distance from $x = 0$ and L respectively, we have in a matrix form,

$$\begin{Bmatrix} F_1 \\ F_2 \end{Bmatrix} = \underbrace{\begin{bmatrix} ik_{lo}(-EA_s + \nu^2 \omega^2 \rho J) & ik_{lo}(EA_s + \nu^2 \omega^2 \rho J)e^{-ik_{lo}L} \\ ik_{lo}(EA_s + \nu^2 \omega^2 \rho J)e^{-ik_{lo}L} & ik_{lo}(-EA_s + \nu^2 \omega^2 \rho J) \end{bmatrix}}_{\Psi} \begin{Bmatrix} A_1 \\ A_2 \end{Bmatrix} \quad (15)$$

Finally, by relating displacement and nodal force, by substituting Eq. (14) into (15) we have the stiffness matrix for the rod Love theory expressed as

$$\begin{Bmatrix} F_1 \\ F_2 \end{Bmatrix} = \underbrace{\Psi \Gamma^{-1}}_{K_{Love}} \begin{Bmatrix} \hat{u}_0 \\ \hat{u}_L \end{Bmatrix} \quad (16)$$

2.3. The spectral element of the Mindlin Herman's rod

Mindlin Herman's rod theory, known as a two-way rod, as well as Love also considers the cross-sectional deformation of the element due to the Poisson effect. It also includes the stresses and axial deformation in the cross sections of the rod as uniform. Figure 2 shows a Mindlin Herman rod model.

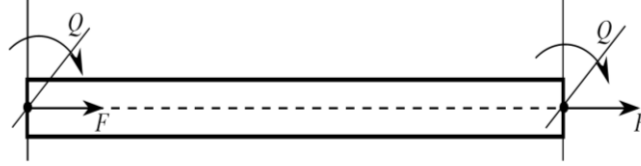


Figure 2. Mindlin Herman rod

For this methodology each node has two degrees of freedom, being longitudinal displacement (u) and transverse displacement (v) where $v = \psi_x y$, ψ represents the transverse contraction. The equations of motion are presented as follows

$$(2\mu + \lambda)A_s \frac{\delta^2 u}{\delta x^2} + \lambda A_s \frac{\delta \psi}{\delta x} = \rho A_s \ddot{u} \quad (17)$$

$$\mu I K_{r1} \frac{\delta^2 \psi}{\delta x^2} - (2\mu + \lambda)A_s \psi - \lambda A_s \frac{\delta u}{\delta x} = \rho I K_{r2} \frac{\delta^2 \psi}{\delta t^2} \quad (18)$$

The constants are found as follows,

$$\mu = \frac{E}{2(1 + \nu)}, \quad \lambda = \frac{\nu E}{(1 + \nu)(1 - 2\nu)}$$

$$K_{r1} = \frac{12}{\pi^2}, \quad K_{r2} = K_{r1} \frac{1 + \nu}{0,87 + 1.12\nu}$$

Transforming to the spectral form, we have the following equations of motion

$$(2\mu + \lambda)A_s \frac{\delta^2 \hat{u}}{\delta x^2} + \lambda A_s \frac{\delta \hat{\psi}}{\delta x} + \omega^2 \rho A_s \hat{u} \quad (19)$$

$$\mu I K_{r1} \frac{\delta^2 \hat{\psi}}{\delta x^2} - (2\mu + \lambda)A_s \hat{\psi} - \lambda A_s \frac{\delta \hat{u}}{\delta x} + \omega^2 \rho I K_{r2} \hat{\psi} \quad (20)$$

Equations can determine the boundary conditions

$$\hat{F}_u = (2\mu + \lambda)A_s \frac{\delta \hat{u}_0}{\delta x} + \lambda A_s \hat{\psi}_0 \quad (21)$$

$$\hat{Q}_\psi = \mu I K_{r1} \frac{\delta \hat{\psi}_0}{\delta x} \quad (22)$$

Since the system presents equations coupled with the dependent variables u, ψ the solutions must be assumed as follows

$$\hat{u} = U e^{-i(\omega t - kx)} \quad (23)$$

$$\hat{\psi} = \Psi e^{-i(\omega t - kx)} \quad (24)$$

By replacing the solutions in the boundary conditions is given the following system

$$\begin{bmatrix} -(2\mu + \lambda)A_s k^2 + \rho A_s \omega^2 & -ik\lambda A_s \\ ik\lambda A_s & -\mu I K_{r1} k^2 - (2\mu + \lambda)A_s + \rho I K_{r2} \omega^2 \end{bmatrix} \begin{Bmatrix} U \\ \Psi \end{Bmatrix} = 0 \quad (25)$$

The wave number k can be obtained from the characteristic equation obtained by the determinant of the system equal presented in eq.(25) so that the polynomial characteristic is

$$a_2 k^4 + a_1 k^2 + a_0 = 0 \quad (26)$$

Where

$$\begin{aligned} a_2 &= \mu A_s I K_{r1} (2\mu + \lambda) \\ a_1 &= [4\mu(\mu + \lambda) + A_s^2 - \rho I K_{r2} \omega^2 (2\mu + \lambda) A_s - \rho A_s \omega^2 \mu I K_{r1}] \\ a_0 &= -\rho A_s \omega^2 [A_s (2\mu + \lambda) - \rho I K_{r2} \omega^2] \end{aligned} \quad (27)$$

Solving the polynomial equation the roots will be,

$$k^2 = \frac{-a_1 \pm \sqrt{a_1^2 - 4a_2 a_0}}{2a_2} \quad (28)$$

Thus, the theory presents two distinct wave numbers being k_1 real and k_2 complex, which means that it is attenuated below its cutoff frequency.

$$\omega_c = \sqrt{\frac{(2\mu + \lambda) A_s}{\rho I K_{r2}}} \quad (29)$$

The longitudinal and transverse displacements are obtained with the following equations

$$\begin{aligned} \hat{u}_x &= A_1 R_1 e^{-ik_1 x} + A_2 R_2 e^{-ik_2 x} - A_3 R_1 e^{-ik_1(L-x)} - A_4 R_2 e^{-ik_2(L-x)} \\ \hat{\psi}_x &= A_1 e^{-ik_1 x} + A_2 e^{-ik_2 x} + A_3 e^{-ik_1(L-x)} + A_4 e^{-ik_2(L-x)} \end{aligned} \quad (30)$$

where R_i is the amplitude ratio given in eq. (30), and the subscript $i=1,2$.

$$R_i = \frac{ik_i \lambda A_s}{-(2\mu + \lambda) A_s k_i^2 + \rho A_s \omega^2}$$

A_1, A_2, A_3 e A_4 constants that can be found by replacing the boundary conditions at nodes $x = 0$ and $x = L$. It gives the following system

$$\begin{Bmatrix} A_1 \\ A_2 \\ A_3 \\ A_4 \end{Bmatrix} = \begin{bmatrix} R_1 & R_2 & -R_1 p_1 & -R_2 p_2 \\ 1 & 1 & p_1 & p_2 \\ R_1 p_1 & R_2 p_2 & -R_1 & -R_2 \\ p_1 & p_2 & 1 & 1 \end{bmatrix}^{-1} \begin{Bmatrix} \hat{u}_0 \\ \hat{\psi}_0 \\ \hat{u}_L \\ \hat{\psi}_L \end{Bmatrix} \quad (31)$$

$$p_1 = e^{-ik_1 L} \text{ e } p_2 = e^{-ik_2 L}$$

By replacing the derivative of the displacement solutions into the boundary conditions where $\hat{F}_u(0) = \hat{F}_1$, $\hat{Q}_\psi(0) = \hat{Q}_1$, $\hat{F}_u(L) = \hat{F}_2$ e $\hat{Q}_\psi(L) = \hat{Q}_2$, we have

$$\begin{Bmatrix} \hat{F}_1 \\ \hat{Q}_1 \\ \hat{F}_2 \\ \hat{Q}_2 \end{Bmatrix} = \begin{bmatrix} -N_1 + M_2 & -N_2 + M_2 & (-N_1 + M_2)p_1 & (-N_2 + M_2)p_2 \\ -ik_1 M_3 & -ik_2 M_3 & ik_1 M_3 p_1 & ik_2 M_3 p_2 \\ (-N_1 + M_2)p_1 & (-N_2 + M_2)p_2 & -N_1 + M_2 & -N_2 + M_2 \\ -ik_1 M_3 p_1 & -ik_2 M_3 p_2 & ik_1 M_3 & ik_2 M_3 \end{bmatrix} \begin{Bmatrix} A_1 \\ A_2 \\ A_3 \\ A_4 \end{Bmatrix} \quad (32)$$

$$M_1 = (2\mu + \lambda) A_s, M_2 = \lambda A_s, M_3 = \mu I K_{r1}, N_1 = ik_1 M_1 R_1, N_2 = ik_2 M_1 R_2$$

The dynamic stiffness matrix of the Mindlin Herman's rod of two modes can be obtained similar to Love's rod by substituting eq.(31) into (32).

2.4. Truss spectral element

As the towers are shaped by rods connected at different angles β , the next step is to transform the energy into expressions involving nodal degrees of freedom relative to the global axes. Thus, it is necessary to apply the rod theories together with a transformation matrix, τ , as

$$\mathbf{S}_t(\omega) = [\tau' \mathbf{S}_b \tau] \quad (43)$$

where \mathbf{S}_b is the dynamic stiffness matrix of the rod. The transformation matrix for the elementary and Love rod is given by

$$\tau = \begin{bmatrix} \cos(\beta) & \sin(\beta) & 0 & 0 \\ \sin(\beta) & \cos(\beta) & 0 & 0 \\ 0 & 0 & \cos(\beta) & \sin(\beta) \\ 0 & 0 & \sin(\beta) & \cos(\beta) \end{bmatrix} \begin{Bmatrix} u_o \\ v_o \\ u_l \\ v_l \end{Bmatrix} \quad (34)$$

and for the Mindlin-Herman rod will be,

$$\tau = \begin{bmatrix} \cos(\beta) & \sin(\beta) & 0 & 0 & 0 & 0 \\ \sin(\beta) & \cos(\beta) & 0 & 0 & 0 & 0 \\ 0 & 0 & 1 & 0 & 0 & 0 \\ 0 & 0 & 0 & \cos(\beta) & \sin(\beta) & 0 \\ 0 & 0 & 0 & \sin(\beta) & \cos(\beta) & 0 \\ 0 & 0 & 0 & 0 & 0 & 1 \end{bmatrix} \begin{Bmatrix} u_o \\ v_o \\ \psi_o \\ u_l \\ v_l \\ \psi_l \end{Bmatrix} \quad (35)$$

3. NUMERICAL ANALYSIS

To validate the models, a test compared to the results for a rod with the same properties, length of 4 m, Young's modulus of 210 GPa, density equals to 7860 kg/m³ and area of 0.02 m². A unitary force imposed at end-left of the rod and receptance measured obtained at right-end in a band of frequency between 0 to 30 kHz.

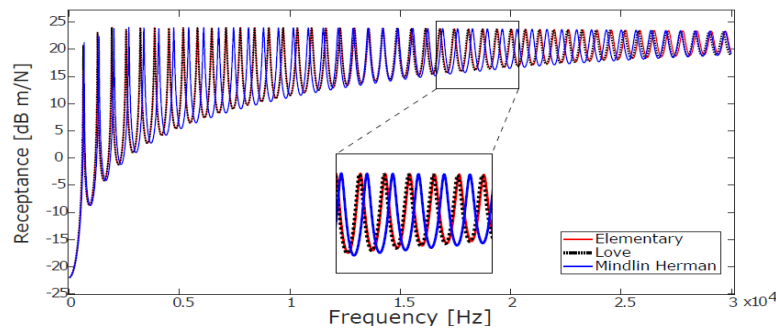


Figure 3: Frequency response function of the elementary, Love, and Mindlin-Herman rods.

Figure 3 shows the comparison of the three rods theories. It is observed that the elementary and Love rods presented greater coherence in their response, while that Mindlin - Herman's rod gives a small difference in low frequencies but increasing in higher ranges. I because since the approach provides a higher number of degrees of freedom associated with the deformation. The influence of the deformation combined with the increase of the Dofs can be seen in the dispersion diagrams displayed in figs. 4 and 5.

In fig. 4 shows the dispersion diagram, which is the wavenumber in the function of the frequency, for the elementary and Love theories. The wavenumber up to the 100 kHz shows good approximation by comparing both methods, but above this frequency, the effect of the lateral contraction influences the propagation and a small divergence is observed as demonstrated in the graphic. In the elementary rod, the non-dispersive propagation maintains during the whole frequency range, however in the Love rod up to the 100 kHz the propagation became dispersive.

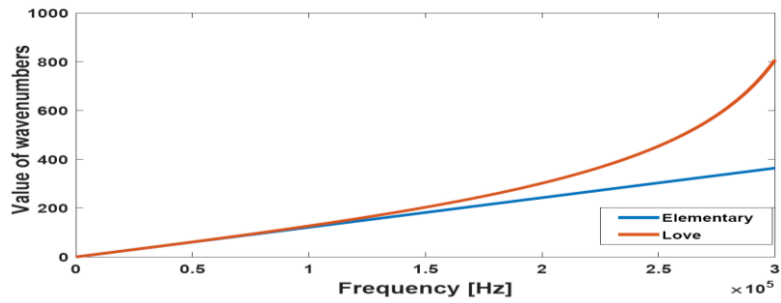


Figure 4: Dispersion curves for elementary and Love theories.

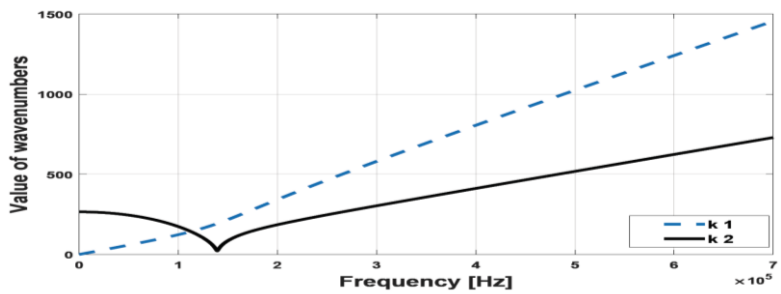


Figure 5: Dispersion curve of the Mindlin Herman theory.

Figure 5 shows the dispersion diagram for the Mindlin Herman theory. In this case, the wave propagation is dispersive. In low frequencies, the first mode approaches the other methods, and the second mode presents a more complex behaviour, where above the cutoff frequency it has real value, so it exhibits propagating behaviour but does not approximate any of the other theories. The computed time for the different theories is presented in Table 1, where it is perceptible a considerable difference in computational time. Table 1 is the computed time of a single rod example presented in fig.3, 4, and 5.

Table-1: Processing Time

Model	Time [s]
Elementary	0.6941
Love	1.0638
Mindlin Herman	1.4402

Next study is the overhead transmission tower. It is modelled as a truss made of steel of elasticity modulus equals to 210 GPa, density of 7860 Kg /m³, and cross-section area of 0.01m. The tower illustrated in fig. 6, is a 26 m height structure composed of 46 rods and 22 nodes. As we are using the SEM, there is no need for discretisation along the rods.

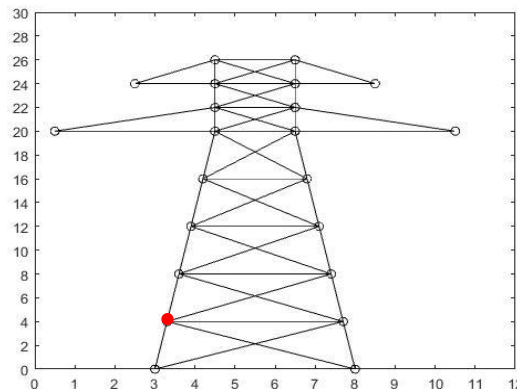


Figure 6. Tower's geometry. The axis of the figure is disposal the dimension in meters.

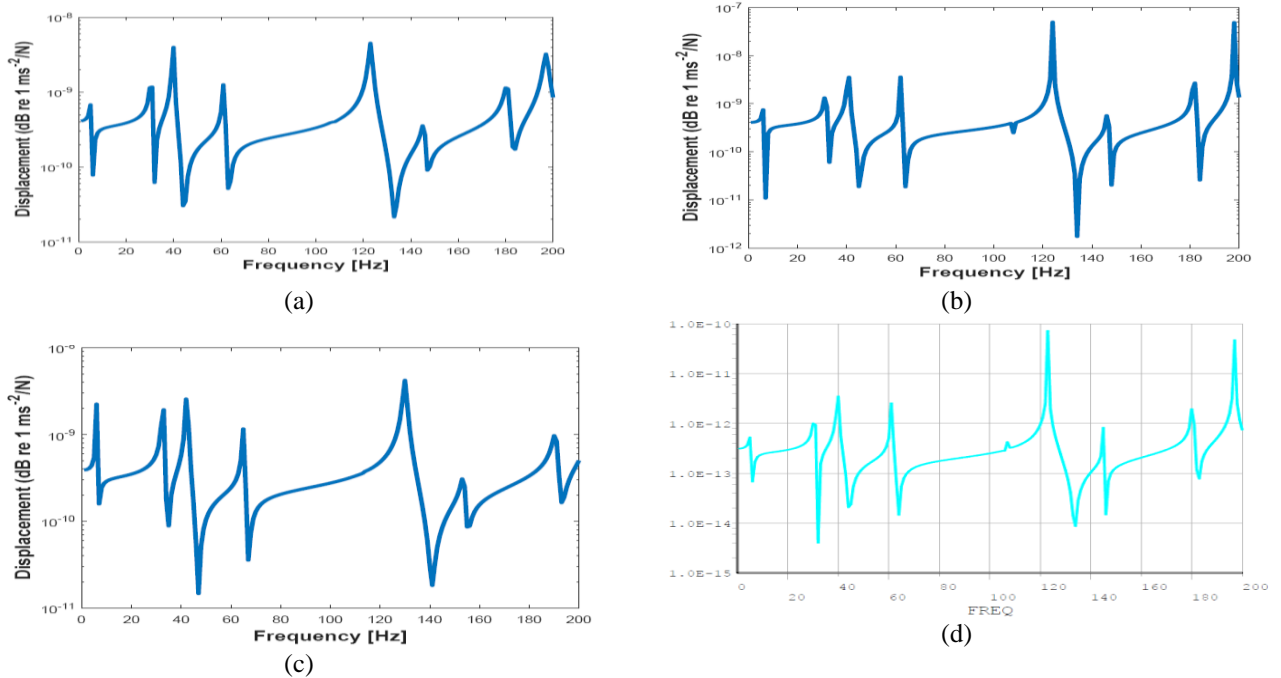


Figure 7. FRF of the tower obtained by (a) Elementary, (b) Love, (c) Mindlin-Herman, (d) Finite Element Method.

The excitation in measured displacement FRFs was calculated in the red node marked in figure 6. FRFs. Figure 7 (a-d) shows the tower FRFs obtained through the three rods theories plus the Finite Element method using ANSYS (element truss180). The FEM analysis was included to validate the study. By comparing the FRFs, the elementary, Love and FEM presented a similar response while the Mindlin-Herman estimate the same resonance frequencies but the mode are slightly different. Again, this approach includes the stresses and axial deformation in the cross sections not considered in the other methods. Table 2 shows the resonance frequencies obtained using the four techniques; all the results obtained a good approximation.

Table 2. Tower Natural Frequencies.

Freq. [Hz]	SEM			FEM discretized 0,01m
	Elementary	Love	Mindlin Herman	
1°	5.6	5.6	5.2	5.6
2°	30.7	30.7	31.8	30.66
3°	39.8	39.8	41.3	39.75
4°	61.2	61.2	64.3	61.14
5°	123.2	123.2	112.5	122.98

The computational time was obtained, using the same computer, under the same conditions, and is shown in Table 3.

Table 3 : Processing Time

Model	Time [s]
Elementary	0.897
Love	2.486
Mindlin Herman	3.374
FEM	108

It is noticed that all the methods had small processing time, but the elementary rod due to its simplicity had time below to the others. Comparing the solution of SEM and FEM, it was noticed the need to discretize in small elements which makes the process computationally much more expensive, demonstrating the needing of a method accurate associated with reduced computational time.

4. CONCLUSION

This work presents a dynamic analysis of a transmission tower using a spectral element method with finite element method validation. To obtain this approximation of the FEM model, a discretization of each tower rod was necessary for 0.01m elements, which shows a higher computational cost in the MEF, with SEM being a great alternative to deal with this analysis, satisfying the reliability requirements and agility in processing. In the analysis performed between the high order rods, the similarity between the responses was remarkable. However the processing for the elementary rod presents less time due to the simplicity of its theory.

5. Referencias

Doyle, J.F., 1997. "Wave propagation in structure: a spectral analysis using fast discrete Fourier Transforms", 2nd ed. *SpingerVerlag*, New York, USA.

Gopalakrishnan, S., Chakraborty, A., & Roy Mahapatra, D. (2007). Spectral Finite Element Method. In *Foundations in Engineering Mechanics*. https://doi.org/10.1007/978-981-10-1902-9_8

Krawczuk, M., Grabowska, J., & Palacz, M. (2006). Longitudinal wave propagation. Part I-Comparison of rod theories. *Journal of Sound and Vibration*, 295(3-5), 461-478. <https://doi.org/10.1016/j.jsv.2005.12.048>

Lam, H. F., & Yin, T. (2011). Dynamic reduction-based structural damage detection of transmission towers: Practical issues and experimental verification. *Engineering Structures*, 33(5), 1459-1478. <https://doi.org/10.1016/j.engstruct.2011.01.009>

Lee, U. (2009). "Spectral Element Method in Structural Dynamics"., *Inha University Press*.

Naidu, G. G., & Krishna, P. M. (2016). *Dynamic Analysis Of Electrical Transmission Tower Using Finite Element Technique*. (November). <https://doi.org/10.13140/RG.2.2.18978.84164>

Nóbrega, E. D., and Santos, J. M. C., 2014. "Method of the spectral element of wave propagation using high order wave guides". *Ibero-Latin American Congress on Computational Methods in Engineering*.

Pereira, F. N. (2009). *Propagação de Ondas e Detecção de Danos com Modelos de Barra de Alta Ordem pelo Método do Elemento Espectral*. Universidade Estadual de Campinas.

Prasad Rao, N., Knight, G. M. S., Lakshmanan, N., & Iyer, N. R. (2010). Investigation of transmission line tower failures. *Engineering Failure Analysis*, 17(5), 1127-1141. <https://doi.org/10.1016/j.engfailanal.2010.01.008>

Taillon, J. Y., Légeron, F., & Prud'Homme, S. (2012). Variation of damping and stiffness of lattice towers with load level. *Journal of Constructional Steel Research*, 71, 111-118. <https://doi.org/10.1016/j.jcsr.2011.10.018>

Yasui, H., Marukawa, H., Momomura, Y., & Ohkuma, T. (1999). Analytical study on wind-induced vibration of power transmission towers. *Journal of Wind Engineering and Industrial Aerodynamics*, 83(1-3), 431-441. [https://doi.org/10.1016/S0167-6105\(99\)00091-4](https://doi.org/10.1016/S0167-6105(99)00091-4)

Krawczuk, M., Grabowska, J., and Palacz, M., 2006. "Longitudinal wave propagation Part II—Analysis of crack influence". *Journal of Sound and Vibration*, vol. 295(3-5), pp. 479-490.

Palacz, M., and Krawczuk, M., 2002. "Analysis of longitudinal wave propagation in a cracked rod by the spectral element method". *Comput Struct* 80 pp. 1809-1816

6. RESPONSIBILITY NOTICE

The authors are the only responsible for the printed material included in this paper.